

Fast Distributed Deep Learning via Worker-adaptive Batch Sizing

Chen Chen¹, Qizhen Weng¹, Wei Wang¹, Baochun Li², Bo Li¹

¹ Hong Kong University of Science and Technology ² University of Toronto

ABSTRACT

Deep neural network models are usually trained in cluster environments, where the model parameters are iteratively refined by multiple worker machines in parallel. One key challenge in this regard is the presence of stragglers, which significantly degrades the learning performance. In this paper, we propose to eliminate stragglers by adapting each worker’s training load to its processing capability; that is, slower workers receive a smaller batch of data to process.

Following this idea, we develop a new synchronization scheme called LB-BSP (Load-balanced BSP). It works by coordinately setting the batch size of each worker so that they can finish batch processing at around the same time. A prerequisite for deciding the workers’ batch sizes is to know their processing speeds before each iteration starts. For the best prediction accuracy, we adopt NARX, an extended recurrent neural network that accounts for both the historical speeds and the driving factors such as CPU and memory in prediction. We have implemented LB-BSP for both TensorFlow and MXNet. EC2 experiments against popular benchmarks show that LB-BSP can effectively accelerate the training of deep models, with up to 2× speedup.

KEYWORDS

Distributed Deep Learning, Batch Size, Load Balancing

1 INTRODUCTION

Due to its computation-intensive nature, deep learning models are typically trained on large clusters in a *distributed* manner [13, 22, 29, 50]: many *worker* machines iteratively refine the model parameters using a subset of training data, i.e., a *sample batch*, and communicate with the *parameter servers* with respect to updates to the model parameters.

While existing distributed training practices [22, 29, 37, 67] are mainly conducted on dedicated clusters with homogeneous workers, we believe that it would become increasingly more common to train new deep learning models using *shared* clusters. Due to their shared nature, these clusters are *heterogeneous* in their hardware configurations and time varying in their resource availability. Naturally, workers running on less capable computing hardware would make slower progress, and have the potential to become *stragglers*.

Stragglers may negatively affect the performance of distributed deep learning training in two possible ways. Each

iteration in the convergence process may need to take a longer period of time; or alternatively depending on the mechanism used for worker coordination, more iterations may be required for convergence. A typical mechanism for worker coordination, for example, is called Bulk Synchronous Parallel (BSP) model. It makes sure that workers are synchronized at the end of each iteration, and the amount of time it takes in each iteration may then be longer as fast workers have to wait for stragglers.

In this paper, we seek to improve the overall performance of distributed training of deep models by reducing the amount of time taken in each iteration, and minimizing the number of iterations at the same time. At a high level, in a shared cluster with a heterogeneous environment, stragglers are mainly caused by the mismatch between the workload and processing capability at each worker, and the intuitive solution is to *apportion* the workload to these workers according to their processing capabilities.

That said, existing load balancing approaches [14, 17, 33, 38] are not suitable for deep learning training. They are designed for cases where each iteration is sufficiently long so that stragglers can be detected and tackled, but iterations in deep learning training are quite short in general, lasting for a few seconds or even less than a second. In fact, it’s unnecessary and even infeasible to address stragglers within iterations. For deep learning workloads, we find it’s more appropriate to detect stragglers at the iteration boundaries, and tackle them by adjusting the size of their sample batches.

In this work, we propose Load-Balanced Bulk Synchronous Parallel (LB-BSP), which adaptively apportions the size of each worker’s sample batch with the objective of equalizing their processing times. This mechanism is referred to as *worker-adaptive batch sizing*. LB-BSP works effectively without introducing the extra overhead of fine-grained progress monitoring or load transfers, and can be easily implemented in modern deep learning frameworks.

While each worker’s processing time increases monotonically as its workload (represented by its batch size) increases, it remains a challenge how each worker’s workload can be accurately apportioned so that the processing times of all the workers can be equalized. We first formulate our objective as a general optimization problem, and then customize the problem further with the specific characteristics of deep

learning training. The result of such customization is a linear optimization problem that can be directly solved.

One prerequisite, however, for solving our optimization problem is the knowledge of each worker’s processing speed of each sample before each iteration runs. Such processing speed may be affected by the available resources, such as CPU and memory. We use the *Nonlinear AutoRegressive eXogenous model* (NARX) [32], an extended recurrent neural network that makes speed predictions with those driving resources accounted.

We have implemented LB-BSP as a Python library that can be integrated in both TensorFlow and MXNet (§4). Our experimental evaluation using benchmark deep learning workloads shows that LB-BSP outperforms the existing mechanisms, especially when resource availability is highly heterogeneous across the workers. In an emulated production cluster built with Google Traces [57], the convergence speed under LB-BSP can be 2× that of BSP. In another GPU-cluster, the performance improvement of LB-BSP over BSP is 41%. With respect to predicting the processing speed, we find NARX surpasses the second best approach by 15%.

2 BACKGROUND AND MOTIVATION

2.1 Distributed Deep Learning

Training process of deep learning models. Deep learning (DL) [48] has dramatically improved the state-of-the-art in many domains such as computer vision [35, 46] and natural language processing [23, 59]. Given a neural network model, the goal of DL training is to find the model parameters ω^* that minimizes the loss function $L(\omega)$ over the entire training dataset, i.e.,

$$\omega^* = \arg \min L(\omega) = \arg \min \frac{1}{|S|} \sum_{s \in S} l(s, \omega). \quad (1)$$

Here S is the labeled training set, and $l(s, \omega)$ is the loss value for a sample $s \in S$ with the current parameters ω .

Mini-batch Stochastic Gradient Descent (SGD) [29, 51] is a popular algorithm to train the model parameters ω^* . Its basic idea is to iteratively update ω with the gradients calculated from sample (*mini-*)batches:

$$\omega^{k+1} = \omega^k - \eta g^k, \text{ where } g^k = \frac{1}{|B^k|} \sum_{s \in B^k} \nabla l(s, \omega^k). \quad (2)$$

Here B^k is a batch sampled from S for iteration k , and η is the *learning rate*. Such an iteration repeats until the model parameters w finally converge.

Distributed deep learning. Due to the ever increasing model complexity and data volume, it has become commonplace to train DL models in a *distributed* manner, with a dedicated *parameter server* (PS) and multiple *workers*. As shown in Fig. 1, in each iteration, each worker i generates

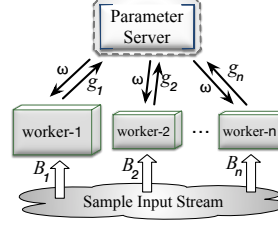


Figure 1: In distributed deep learning, workers iteratively refine model parameters with sample batches generated from the input stream.

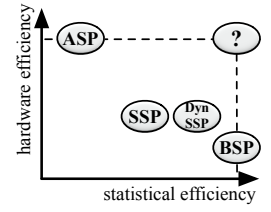


Figure 2: Performance comparison of existing worker-coordinating schemes in face of non-transient stragglers.

a sample batch B_i from its input stream, based on which it then calculates the gradient g_i with the latest global model parameters ω .

Distributed DL training has been conducted in various cluster environments. Here we broadly classify those clusters into two types: *dedicated* clusters and *non-dedicated* clusters.

1) Dedicated clusters usually consist of homogeneous workers and are monopolized by only one training job. Dedicated clusters are typically used by production service providers or model developers, to whom fast model convergence is of the highest priority.

2) Non-dedicated clusters are usually built from *heterogeneous* machines in which DL workloads coexist with other data analytic workloads. Non-dedicated clusters are typically adopted by cost-sensitive organizational entities or budget-limited individuals. For example, large-scale shared clusters [25, 57] often span multiple machine generations or specifications, with *dynamic, low* resource utilization in general; to reduce resource wastage due to over-subscription, the cluster operator can run long-lasting, delay-tolerant DL workloads in the background, using the leftover resources. Besides, in a DL training work, a user might want to combine the use of multiple GPUs with different computing capabilities—mainly because they are the only accessible ones or among the cheapest in EC2 spot market [2]. We expect that, with the increasing popularity of DL, more training work would be conducted in non-dedicated clusters.

The two types of clusters differ significantly with regard to the straggling factors. In dedicated clusters, all workers have a similar computation capability, and the stragglers are usually *transient*. However, in non-dedicated clusters with heterogeneous hardware or dynamic resources, workers’ computational capabilities can be highly different. The resultant straggling factors are usually *non-transient* and *salient*, in face of which, as we show next, the distributed DL process would suffer remarkable performance degradation.

2.2 Existing Coordinating Schemes

Given the prevalence of stragglers, how to coordinate workers critically affects the learning performance. Several Coordinating schemes have been developed in this regard: Bulk Synchronous Parallel (BSP), Asynchronous Parallel (ASP), Stale Synchronous Parallel (SSP) and its extension DynSSP. However, they all have limitations in the presence of stragglers in non-dedicated clusters.

Bulk Synchronous Parallel. In BSP, workers *synchronize* at the end-of-iteration *barrier* and cannot proceed until the model parameters have been fully updated by *all* workers. This ensures the computation to use *up-to-date* parameters, which in turn yields *high-quality model refinement* in each iteration. The BSP model hence achieves *optimal statistical efficiency* with correctness guarantees. However, synchronous execution results in *low hardware efficiency*: fast workers have to wait for stragglers to complete in each iteration, wasting computing cycles and delaying the training progress.

Asynchronous Parallel. To avoid resource wastage, many learning problems are solved in the ASP model, where workers *asynchronously* proceed to the next iteration before the parameters have been fully updated. The ASP model wastes *no* computing cycle and attains *highest* hardware efficiency. However, the price paid is *low* statistical efficiency: without synchronization, the computation often uses *stale* parameters, which may require much more iterations to converge and yield low-quality updates that poison the learning performance [41, 47].

Stale Synchronous Parallel. The SSP model [26, 41] comes as a middle ground between BSP and ASP. In SSP, fast workers synchronize with stragglers *only when* the *staleness* of parameters (the number of missing updates) is about to exceed a bounded amount. In this way, SSP can accelerate the learning process while providing convergence guarantee. Nonetheless, SSP targets mainly at *transient* stragglers, and it assumes that stragglers can soon catch up with others in later iterations. But in non-dedicated clusters, the *non-transient* stragglers hold across many consecutive iterations, so the staleness allowance would be easily used up, and the fastest worker would have to wait for the slowest one almost after each iteration. This leads to exactly the same problem as BSP—*low hardware efficiency*.

DynSSP. The recently proposed DynSSP [44] is built upon SSP, and it incorporates heterogeneity-aware dynamic learning rate to achieve improved *statistical efficiency*. However, because it has same *hardware efficiency* as SSP, it also behaves poorly facing *non-transient* stragglers.

In a nutshell, when faced with non-transient stragglers, distributed DL process would always be slowed down—suffering either *low hardware efficiency* or *low statistical efficiency*, as

shown in Fig. 2. Hence, for optimal performance in both worlds, we shall eliminate those non-transient stragglers.

The root cause of non-stragglers is that *existing DL systems blindly enforce a fixed load (i.e., batch size) on all workers—regardless of their hardware heterogeneity or resource variations*. Hence, to eliminate stragglers is actually to *load-balance* the workers based on their processing capabilities.

2.3 Load-balancing DL workloads

In typical load balancing approaches, there are two basic steps: first to *detect* stragglers, and second to *tackle* stragglers by load adjustment. For example, FlexRR [38], a recently proposed load-balancing approach for Machine Learning workloads, detects stragglers by frequently measuring and synchronizing the worker progress at runtime; once stragglers are detected, it immediately offloads some of their training work to other lightly-loaded workers.

However, such *intra-iteration* approaches won't work well when extended to DL workloads. To load-balance DL workloads, we will show that, a much more efficient and practical way is to adjust each worker's load, i.e., its *batch size*, at the iteration boundaries. Here we justify that with the following properties of DL workloads:

- **[P1] Short iterations.** DL iterations are usually very *short* [13, 21, 37], because the sample batches shall be small enough to avoid sacrificing the learning efficiency [18, 51]. This rules out the *intra-iteration* straggler detecting and load transferring steps as adopted in FlexRR, which are too time-consuming and meanwhile bring non-negligible computation and communication overheads.
- **[P2] Strong iterative-ness.** DL training process is composed of thousands of iterations sharing the identical training operations. When analyzing a worker's progressing state, historical information in the past iterations plays as a valuable reference.
- **[P3] Load inner-homogeneity.** For DL workloads, each training sample consumes a *fixed* number of CPU cycles, which is totally determined by the pre-defined DL model. Therefore, the batch size *accurately controls* the iteration load. This is different from traditional workloads, like SQL queries running under MapReduce [30] or Spark [64], where the additional load brought by one data item is not constant but dependent to the item *value* (e.g., whether the *key* is *selected* for further processing).
- **[P4] Load indivisibility.** From an *engineering* perspective, adjusting DL loads at runtime is actually *infeasible*. In state-of-the-art DL frameworks like TensorFlow [13], MXNet [21] and Caffe [43], all samples in the input batch would be processed *not one by one* but—for fast processing speed—as an *indivisible matrix*, e.g., a tensor in TensorFlow or a NDAarray in MXNet. The size of such matrix, i.e., the worker's load, is fixed during the iterations.

t	batch processing time	x_i	batch size on worker- i
t^p	computation time	t^m	communication time
$\Gamma(\cdot)$	function of x and t_p	v	sample processing speed
\dot{x}	initial batch size	X	$n\dot{x}$ (n is worker number)

Table 1: Summary of important notations.

The above DL properties indicate that stragglers *shall* and *could* be detected at the iteration boundaries, and meanwhile *batch size* is an ideal tool to adjust the loads of workers. This motivates our load-balancing solution, *worker-adaptive batch sizing*, which will be elaborated in following sections.

3 LOAD-BALANCED BSP

In this section, we introduce *Load-balanced Bulk Synchronous Parallel* (LB-BSP), a BSP-based worker-coordinating scheme for distributed DL. The basic intuition of LB-BSP is to *adaptively adjust the batch size of each worker so as to equalize their batch processing times*. We first formulate the problem, and then respectively elaborate our solutions for CPU-clusters and GPU-clusters.

3.1 Problem Formulation

By *batch processing time*, we refer to the time spent on the whole procedure that a worker *pulls* model parameters from the PS, *calculates* the gradient from its sample batch, and finally *pushes* it to the PS. Here we divide the *batch processing time* (t) into the following two parts:

- *computation time* (t^p)—the time taken to compute gradient from the sample batch. Under a given environment, it monotonously increases with the worker batch size.
- *communication time*¹ (t^m)—the time taken to transmit parameters/gradient from/to the PS. The transmission amount is decided by the DL model, irrespective of the batch size.

With LB-BSP, our objective is to equalize the batch processing time by right-sizing the batches for each worker. This objective can be described as an optimization problem. That is, given n workers with initial batch size \dot{x} , we want to find the worker batch sizes $\vec{x} = (x_1, x_2, \dots, x_n)$ that can minimize the maximal batch processing time among all workers:

$$\begin{aligned}
& \text{Min}_{\vec{x}=(x_1, x_2, \dots, x_n)} \quad \max_{i \in \{1, 2, \dots, n\}} t_i, \\
& \text{s.t.} \quad t_i = t_i^p + t_i^m, \quad i = 1, \dots, n; \\
& \quad \quad t_i^p = \Gamma_i(x_i), \quad i = 1, \dots, n; \\
& \quad \quad \sum_{i=1}^n x_i = X.
\end{aligned} \tag{3}$$

Here $\Gamma_i(\cdot)$ is the function between worker- i 's computation time t_i^p and its batch size x_i ; by the last constraint where

¹Communication and computation might be partially overlapped under TensorFlow and MXNet [67]; for clarity, the communication time in our definition excludes the overlapped periods.

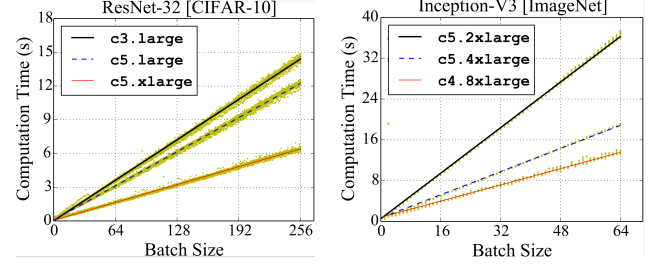


Figure 3: The relationship between computation time and batch size for different EC2 instance types.

$X = n\dot{x}$, we want to ensure that the total number of samples processed in each iteration is the same as in vanilla BSP. Table 1 summarizes the important notations.

Next, we will customize and solve this optimization problem respectively for CPU-clusters and GPU-clusters, based on their particular execution characteristics.

3.2 LB-BSP in CPU-clusters

CPU-clusters refer to those clusters without any computing accelerators like GPUs. Although training with CPU is slow, it still shares the DL market due to the prevalence of idled CPU resources and the scarcity and expensiveness of GPUs [22, 29]. For CPU-clusters, the initial optimization problem can be simplified from the following aspects:

1) $t^p \gg t^m$ ($t \approx t^p$). On CPU-workers, the *forward/backward propagation* for gradient calculation is usually computational intensive [40]. In our EC2 measurements, when training Inception-V3 model on ImageNet dataset with 32 c5.2xlarge instances, the computation time t^p takes up more than 99% of the batch processing time t . Thus, as a reasonable approximation, we can consider t^p as t .

2) $\Gamma(x) = x/v$. In a DL iteration, all the samples share the identical training operations and consume a fixed amount of CPU cycles. Therefore, the computation time t^p is strictly *proportional* to the batch size. To further confirm that, we respectively train the ResNet-32 and Inception-V3 model (introduced in §5.1) with different types of EC2 instances. We vary the batch size x and record the corresponded computation time t^p in Fig. 3. The measurement results suggest strong linearity between x and t^p in each case. Let v be the ratio of x to t^p , i.e., the *sample processing speed*, then we have $t^p = \Gamma(x) = x/v$.

Given the above simplifications, we can easily get the solution to the optimization problem described in Eq. 3: $x_i = \frac{v_i}{\sum_{j=1}^n v_j} X$. Hence, to get the targeted batch size on each worker, we only need to know their sample processing speeds.

However, in typically non-dedicated environments—like training with the leftover resources of shared clusters, the sample processing speed is not a constant but varies with

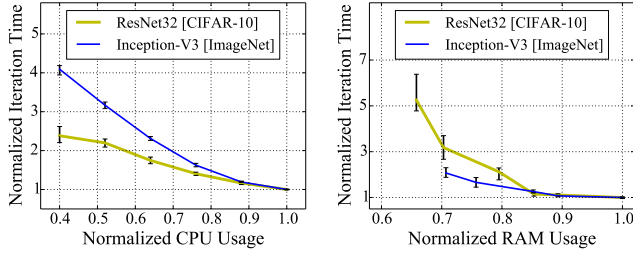


Figure 4: Sample processing speed would be slowed down with fewer CPU/RAM resources. The resource usage and iteration time are normalized by the monopolizing case. Each point is an average of 100 iterations. Experiments are done with the stress-ng tool [8] on c5.2xlarge instance with swap spaces.

the available resources. Because batch size must be specified priori to each iteration (§2.3), we need to predict each worker’s sample processing speed before the iteration starts.

3.2.1 Predicting Sample Processing Speed.

Accurate speed prediction is *important* but *difficult*. When training DL models at a large scale under LB-BSP, the prediction error for merely one worker could delay all other workers. Speed prediction is also challenging, because non-dedicated CPU-clusters usually suffer both *transient* and *non-transient* stragglers: ideally, a good prediction approach shall *be robust to random perturbations, and can meanwhile agilely react to the resource variations*. We have surveyed a series of prediction technologies, and finally find NARX [32, 36] is the most appropriate one.

Potential methods. An intuitive prediction approach is to simply use the speed of the last iteration as the predicted speed for the iteration to start. However, this approach is not robust to temporary speed perturbations. Another intuitive approach is to use the Exponential Moving Average (EMA) as the predicted speed. This approach, by considering the older speeds with an exponentially decreasing weights, is robust to transient fluctuations. However, EMA fails to react timely to sharp speed changes caused by sudden resource variations.

The speed prediction problem facing us is basically a classical research problem—*time series prediction*, for which many *statistical* or *learning based* techniques have been proposed. The typical *statistical* approach is *Autoregressive Integrated Moving Average* (ARIMA) [34], which makes predictions based on statistics likes moving average and the variation of deviations. Later on, models based on *Recurrent Neural Network* (RNN) [24] (like plain RNN and LSTM [42]), due to their ability to maintain inner memory, have been applied

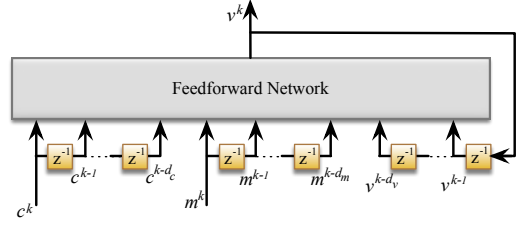


Figure 5: NARX architecture.

in forecasting real-world time series like stock price [56] or transport flow [55].

However, for our problem, the prediction performance of all the above approaches is limited by their *blindness* to underlying resources. Actually, the sample processing speed varies with the CPU/memory resources. This is supported by Fig. 4, in which the DL processes are slowed down after we restrict their resource usage. Taking those driving resources into consideration can help to distinguish the non-transient stragglers from the random perturbations. We find that the *Nonlinear AutoRegressive eXogenous* (NARX) model [32, 36] is a good fit for that purpose.

NARX. The NARX model we use is basically an extended recurrent neural network that takes three series as inputs: past values of sample processing speeds (\mathbf{v}), current and past values of the two *driving* resources: CPU/memory usage (\mathbf{c}/\mathbf{m}). Essentially, NARX aims to learn a *nonlinear function* $F(\cdot)$ between predicted speed and a limited view (specified with a *look-back window*) of the input series:

$$v^k = F(v^{k-1}, \dots, v^{k-d_v}, c^k, \dots, c^{k-d_c}, m^k, \dots, m^{k-d_m}). \quad (4)$$

Here v^k , c^k and m^k respectively represents the value of *speed*, *CPU* and *memory* usage in iteration k ; d_v , d_c and d_m represent the corresponded *look-back window size* of each series. Fig. 5 shows the unfolded architecture of NARX, in which the values of each series within the look-back window are fed into a *feedforward* neural network.

In practice, to ensure high prediction accuracy, we maintain a NARX model for each worker, which is trained online with the incrementally collected execution data (i.e., \mathbf{v} , \mathbf{c} and \mathbf{m}). To avoid high model complexity, as in other prediction works [16, 19], the *look-back window* sizes for all the three input series are set to 2, and we include only *one* hidden layer in the feedforward network. Such a simple NARX model, with *less than 20* parameters, can avoid over-fitting and achieve fast convergence. In practice (§5.4), we find it can meanwhile make predictions accurate enough, beating all those potential approaches we surveyed.

3.3 LB-BSP in GPU-clusters

Training DL models in GPU-clusters, i.e., with GPU-equipped workers, is prevalent due to their strong parallel processing

capabilities [37, 67]. Compared with CPUs, GPUs have much more kernels for concurrent data processing. Thus, the relationship between a GPU-worker’s computation time t^p and its batch size x is more complicated.

To demystify the relationship $\Gamma(\cdot)$ between t^p and x for GPU-workers, we have conducted a series of measurements in EC2 GPU instances, as shown in Fig. 6. The models we run are a 7-layer Convolutional Neural Network and Inception-V3; the revealed relationships are all *non-linear*. In particular, we have following observations:

1) Minimum Saturation Point (x^s)—the threshold of batch size x below which the computation time t^p would be almost constant. That point x^s exists because, when x is too small that only a portion of the parallel computing kernels are utilized, GPU would be *unsaturated* and those busy kernels then dominate t^p [49, 52]. Generally, x^s would be smaller for datasets with larger samples or more complicated DL models. Setting x smaller than x^s unnecessarily wastes resources and meanwhile does not help reduce t^p , so the optimal solution of x would always be *no less* than x^s .

2) Out-Of-Memory Point (x^o)—the threshold of x above which the GPU would encounter *Out-Of-Memory* error. During GPU computing, the data must reside on the GPU DRAM, which is fast but limited [53, 62]. To avoid the Out-Of-Memory error, x must be set *no larger* than x^o .

3) Linearity between x^s and x^o . Within the interval $[x^s, x^o]$, the computation time t^p in both figures increases *linearly* with x . Let m be the line slope and b be the intercept, then we have $t^p = \Gamma(x) = m * x + b$.

Those observations are consistent with our later measurements for ResNet-32 (Fig. 12 in §5.5). Therefore, for GPU-clusters, the *non-linear* constraint $t_i^p = \Gamma_i(x_i)$ in Eq. 3 can be equivalently translated into the following *linear* constraints:

$$\begin{aligned} t_i^p &= m_i * x_i + b_i, \quad i = 1, \dots, n; \\ x_i^s &\leq x_i \leq x_i^o, \quad i = 1, \dots, n; \end{aligned} \quad (5)$$

Then, how to obtain the coefficients in the updated constraints— m_i, b_i, x_i^s, x_i^o —to solve the optimization problem? After surveying the current use cases of GPU, we find that fine-grained GPU sharing is very *rare*, due to the technical difficulties and large overheads [4]. For TensorFlow, shared use of GPU is *not* currently or even planned to be supported [3]. Therefore, we can limit our focus to cases where one GPU is dedicated to one DL work.

Performance of a dedicated GPU is *stable*, as indicated by Fig. 6, where the measurement in each case spans for 5 hours. Therefore, in GPU-clusters we don’t need to make online predictions for the coefficients m_i, b_i, x_i^s, x_i^o : they can be obtained by offline profiling or with a fast profiling phase at the beginning of the training process.

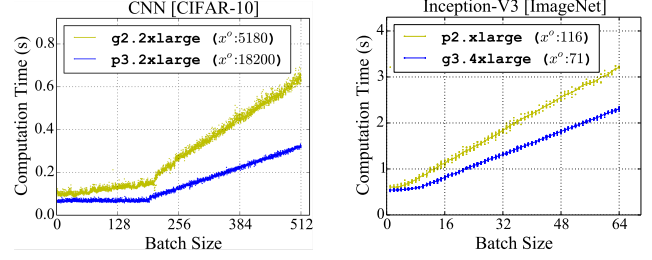


Figure 6: The relationship between computation time and batch size on different GPU instances (values in the legends are the Out-Of-Memory Points).

Additionally, because a GPU-worker is typically tens of times faster than a CPU-worker, the communication time t^m in GPU-clusters is *no longer* negligible. Thus it shall be predicted for each iteration. Different from the speed prediction problem in §3.2.1, for dedicated GPU-workers there are no evident driving factors for t^m , and meanwhile the external network state is relatively stable during the much *shorter* GPU iterations, so for simplicity we can use EMA for t^m estimation.

After we have obtained all those coefficients and the predicted communication time t^m , the resultant *linear* optimization problem can be easily solved with existing mathematical toolboxes.

3.4 Weighted Gradient Aggregation

Recall that our objective under LB-BSP is to simultaneously achieve best hardware efficiency and statistical efficiency. By solving the optimization problem in Eq. 3, we eliminate resource wastage and realize the first part—best hardware efficiency as ASP. Next, we show that with weighted gradient aggregation, LB-BSP can also make the second part—best statistical efficiency as BSP.

One obstacle facing LB-BSP is that workers have different batch sizes under it. Due to such heterogeneous batch sizes, the naively aggregated gradient would be *biased*, impairing the statistical efficiency. We will first elaborate that problem and then propose *weighted gradient aggregation* to solve it.

Naive aggregation causes biased gradient under LB-BSP.

Under BSP, the aggregated gradient g for parameter updating is the naive average of the gradients from workers. Suppose there are n workers and g_i is the gradient calculated on worker- i ($i=1, 2, \dots, n$), then

$$g = \frac{1}{n} \sum_{i=1}^n g_i, \quad \text{where } g_i = \frac{1}{|B_i|} \sum_{s \in B_i} \nabla l(s, \omega). \quad (6)$$

Here B_i is the batch on worker- i . Getting rid of g_i , we have

$$g = \frac{1}{n} \sum_{i=1}^n \frac{1}{|B_i|} \sum_{s \in B_i} \nabla l(s, \omega) = \sum_{i=1}^n \sum_{s \in B_i} \frac{1}{n|B_i|} \cdot \nabla l(s, \omega). \quad (7)$$

This implies that, when workers have different batch sizes ($|B_i|$) under LB-BSP, the *ponderance* of different samples in parameter updating, i.e., $\frac{1}{n|B_i|}$, is also different. This violates the DL principle that *each sample shall be treated equally in the training process*, and the resultant gradient g is biased to samples in small batches.

Weighted Gradient Aggregation. To avoid biased gradient, we propose *weighted gradient aggregation*—using a worker’s batch size as the weight when aggregating its gradient. Then, suppose the total batch size $\sum_{j=1}^n |B_j| = X$, we have

$$g = \frac{1}{\sum_{j=1}^n |B_j|} \sum_{i=1}^n |B_i| \cdot g_i = \sum_{i=1}^n \sum_{s \in B_i} \frac{1}{X} \cdot \nabla l(s, \omega). \quad (8)$$

Obviously, each sample always plays an equal role in parameters updating, regardless of the batch size heterogeneity. After the fix, LB-BSP has following properties:

1) **No parameter staleness.** With barriers, LB-BSP ensures that all workers share the latest model parameters.

2) **Identical per-iteration progress as BSP.** As a constraint in Eq. 3, the total number of samples processed in each iteration under LB-BSP is the same with BSP.

3) **Unbiased gradient.** With weighted gradient aggregation, the model is updated with the *unbiased average* of gradients from all the samples processed in the iteration.

Given the above properties, for training dataset satisfying the *i.i.d.* requirement, i.e., samples being *independent* and *identically distributed*, LB-BSP can always achieve the identical statistical efficiency with BSP, which is known to be optimal. This will be confirmed in our later evaluations.

3.5 Discussions

Worker-adaptive batch sizing in ASP. Although LB-BSP is built upon BSP, its basic philosophy of worker-adaptive batch sizing can also be integrated into ASP to avoid stale parameters. Nonetheless, under ASP every worker proceeds independently without barriers, so it’s hard to *simultaneously* and *coordinately* adjust worker batch size, leading to a performance worse than LB-BSP.

Uneven sample access frequency. In distributed DL, a worker may have access to the *whole* or only a *shard* of the training dataset. In the latter case, under LB-BSP, when faster workers keep training with larger batches, samples in their data shards would be accessed more frequently, leading to *biased* training results if the initial dataset is not well shuffled. Actually this problem *widely exists under each worker-coordinating scheme*. For example, under BSP, when the training datasets are not equally partitioned among workers, samples in small shards would be accessed more frequently; under ASP, similar with LB-BSP, samples possessed by faster

Algorithm 1 LB-BSP workflow for CPU-clusters

Worker: $i=1, 2, \dots, n$:

- 1: **procedure** WORKERITERATE(k)
- 2: pull w^k from PS
- 3: push v_i^{k-1}, c_i^k, m_i^k to BatchSizeManager and pull $|B_i^k|$
- 4: load the next data batch B_i^k
- 5: calculate local gradient g_i^k
- 6: $\bar{g}_i^k \leftarrow \frac{n|B_i^k|}{X} g_i^k$, push to PS $\triangleright \bar{g}_i^k$: weighted gradient

Parameter Server (PS):

- 1: **procedure** PARAMETERSERVERITERATE(k)
- 2: aggregate gradient $g^k \leftarrow \frac{1}{n} \sum_{i=1}^n \bar{g}_i^k = \frac{1}{X} \sum_{i=1}^n |B_i^k| g_i^k$
- 3: update parameters $w^{k+1} \leftarrow w^k - \eta g^k$ $\triangleright \eta$: learning rate

BatchSizeManager:

- 1: **procedure** BATCHSIZEMANAGERITERATE(k)
 - 2: predict $v_1^k, v_2^k, \dots, v_n^k$ with NARX models
 - 3: calculate $|B_i^k|$ based on $v_i^k, i = 1, 2, \dots, n$
 - 4: **procedure** TRAINNARXONLINE
 - 5: maintain the series of v, c, m
 - 6: take turns to train each NARX models at low priority
-

workers would be trained with more frequently. We will address this problem in our subsequent work.

End-of-iteration network burst. One well-known problem of BSP is the end-of-iteration network burst: in GPU clusters, when many workers communicate with the PS simultaneously at the barrier, the network would be a bottleneck. This problem is orthogonal to our work, and the methods proposed by other works like Poseidon [67] can be adopted to mitigate that bottleneck.

4 IMPLEMENTATION

Our LB-BSP implementation pursues following objectives:

- **Generally applicable.** We want LB-BSP to be pluggable for multiple DL frameworks. Thus, we implement its core algorithm in a separated Python Library, BatchSizeManager, which is applicable for both TensorFlow and MXNet.
- **Light-weight.** We want to minimize the overheads of LB-BSP on normal DL process. So we adopt a series of techniques like non-blocking batch-size updating, Thrift RPC, NARX model reuse, etc.

Fig. 7 shows the LB-BSP architecture for CPU-clusters and Alg. 1 describes the detailed workflow. At the start of iteration k , each worker pushes its execution states (last sample processing speed v^{k-1} , current CPU/RAM usage c^k/m^k) to the BatchSizeManager and pulls the new batch size $|B^k|$.

The LB-BSP implementation for GPU-clusters shares a similar architecture, but the reported worker state is the communication time and the batch sizes are calculated without NARX models. Moreover, while the batch size updating

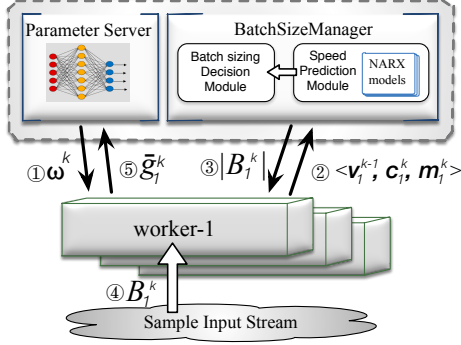


Figure 7: LB-BSP procedures for CPU-clusters in iteration k . Circled numbers mean execution order.

process (②&③ in Fig. 7) is *blocking* in CPU-clusters so that the BatchSizeManager can get the latest states, it is *non-blocking* in GPU-clusters, which are usually less dynamic (§3.3), to avoid prolonging the very short and communication-intensive iterations. For that purpose, in each GPU-worker we launch a separated thread to update the batch size in the background. In the remaining part, we will focus on the LB-BSP implementation in CPU-clusters.

4.1 Batch Size Management Framework

Collecting execution states from workers. To realize LB-BSP, at the worker side, we need to obtain the sample processing speed and the temporal CPU/memory usage. Calculating sample processing speed requires the knowledge of exact computation time. This is particularly challenging for TensorFlow due to its design philosophy of “*deferred execution*”. We choose to profile the computation time from the Timeline [11] object after each iteration finishes, by measuring the makespan of all the Tensorflow *operations* related to gradient computation. Besides, to measure the CPU/memory usage, we resort to Python psutil [6] library.

Thrift RPC communication. In practice we co-locate the BatchSizeManager and the PS in one physical machine, because the PS is actually idle in most time. For efficient communication between BatchSizeManager and workers, we employ Apache Thrift [1], a RPC protocol developed by Facebook for scalable cross-language communication. In particular, each worker calls the following RPC function to get the updated batch size:

```
new_batch_size = rpcClient.update_batch_size(
    taskid, last_speed, cpu_usage, memory_usage)
```

After receiving the RPC calls, BatchSizeManager would use the NARX models to make speed predictions and decide each worker’s batch size for balanced loads. Yet, one challenge is how to *efficiently* train the NARX models online, with the incrementally collected execution information, which will be addressed next.

4.2 Online NARX Training

In our implementation, the NARX models are written in Keras [5], a high-level neural network API. Because accurate NARX training requires enough input samples (one sample corresponds to one DL iteration), we use the NARX models for prediction *only after the first 500 iterations*. In practice we find that 500 samples are enough for accurately training our NARX models, which are quite simple (§3.2.1). Within the first 500 iterations, we can use EMA or, if that DL job is recurring, the past NARX models trained in former runs.

Moreover, for fast convergence, parameters of the NARX models are initialized by reusing available pre-trained models, even though those models are trained for other workers or DL applications. Such a model-reuse approach has been shown [63] to largely speed up the model convergence. Besides, we enable early stopping in the training process. That training process would stop if the loss value reduces *less than 0.0001 for 4 consecutive steps*. Furthermore, to pursue low overhead, we train the NARX models in *separated threads with low priority* (the priority is explicitly specified through Python Threading2 library [7]), and models of different workers are trained in a *round-robin* manner—at any time the number of models that can be trained concurrently is limited to half of the total number of CPU cores.

5 EVALUATION

Our evaluation seeks to answer the following questions:

- **How does LB-BSP perform on DL convergence?** In face of non-transient stragglers (§5.2), LB-BSP outperforms all existing schemes by being optimal in both hardware efficiency and statistical efficiency. In an emulated production cluster (§5.3), it can speed up the DL convergence by more than 2×. In another GPU-cluster (§5.5), it can well adapt to the network variation and improve the hardware efficiency by around 41%, compared with BSP.
- **How effective is the NARX prediction approach?** By diving deep into the speed prediction results (§5.4), we confirm that NARX is robust to random variations and can meanwhile react promptly to non-transient stragglers; as a result, it brings a convergence speed 15% better than that with the second best approach.
- **How about the extra overhead of LB-BSP?** We evaluate how the batch adjusting process would prolong the iteration time in clusters of different scales (§5.6). That gap is less than 1.1% even in a large cluster with 96 workers.

5.1 Experimental Setup

Experimental Platforms. We conduct our experiments on three different Amazon EC2 clusters. **Cluster-A**, for experiments with finely-controlled stragglers, is composed of 1 PS server (c5.4xlarge) and 32 workers (c5.2xlarge), each

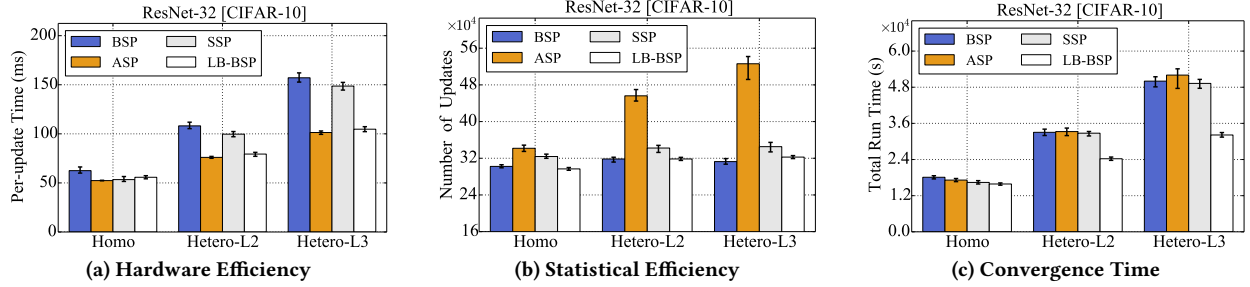


Figure 8: Performance with CIFAR-10 workloads.

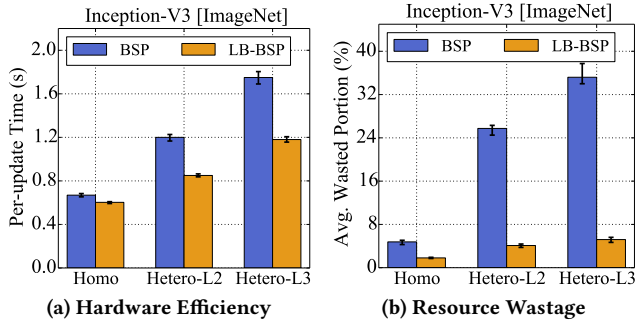


Figure 9: Performance with ImageNet workloads.

worker having 8 cores and 16GB memory. We include 32 workers in the cluster because it’s a reported scale at which distributed DL applications empirically benefit most [67]. **Cluster-B** contains 32 worker nodes of different types to emulate the production environment. **Cluster-C** is a heterogeneous cluster with 8 GPU-instances, used for evaluating LB-BSP in GPU-clusters. Operating system of all the instances is 64-bit Ubuntu Server 16.04 LTS (HVM). For generality, in Cluster-A and Cluster-B we run TensorFlow, while in Cluster-C we run MXNet.

Datasets and Models. We use two typical image classification datasets. (1) CIFAR-10 [45], a dataset containing 50K 32×32 colored images of 10 classes; (2) ILSVRC12 [58], a subset of ImageNet22K that has 1.28 million of training images in 1000 categories. On CIFAR-10 dataset, we train the ResNet-32 model, a 32-layer *deep residual* neural network [39]; on ImageNet dataset, we train the Inception-V3 model [9], an improved version of GoogleLeNet [60]. The initial batch size of each worker is set to 128 for ResNet-32, and 32 for Inception-V3. Meanwhile, the initial learning rate is set to 0.1 for ResNet-32, and 0.045 for Inception-V3. All those hyper-parameters are the default settings in the TensorFlow official github repository [10].

Metrics. The model training efficiency is quantified as the runtime required to converge to a given tolerance. It’s further decoupled into two aspects: statistical efficiency and hardware efficiency. Statistical efficiency is measured as the number of updates (gradients) the PS receives until model

convergence, and hardware efficiency is measured as the *per-update time*—the average time each update takes.

Schemes Compared. We compare LB-BSP directly with BSP, ASP, SSP, and indirectly with DynSSP. TensorFlow currently only support ASP and BSP, so we implemented SSP with a plugged worker-coordinator, which will dictate the fastest workers to wait as long as the staleness threshold is reached. For DynSSP, we didn’t implement it because its underlying data structure is not open-sourced for TensorFlow or MXNet, but we can *indirectly* justify the performance relationship between DynSSP and LB-BSP, bridged by BSP and SSP. Note that FlexRR is not compared because it assumes divisible loads and is simply incompatible with TensorFlow or MXNet (§2.3).

5.2 Results with Fine-tuned Stragglers

Straggler Injection. We use Cluster-A to evaluate the performance of LB-BSP in different heterogeneity levels. For that purpose, we inject artificial stragglers by running on each worker a *competing process*; that process consumes designated cpu cycles and memory space. In particular, to realize dynamicity, we make that competing process periodically run or sleep with certain probability; to realize heterogeneity, in different workers that probability and the resource consumption of the competing process are different. By tuning those configurations, we create three heterogeneity levels: Homo—no stragglers at all; Hetero-L2 (L3)—sample processing speed of the slowest worker is roughly 1/2 (1/3) of the fastest one.

CIFAR-10 Results. Fig. 8 shows the performance under different synchronization schemes when training ResNet-32 model on CIFAR-10 dataset. Here the training process converges, in our definition, *when the loss function is below the targeted value (0.6) for 10 consecutive iterations*. Besides, in SSP the *staleness threshold* is set to 10 iterations (*clocks*). Moreover, we repeat each training process for 3 times, and report min/max value of each metric via error bars.

As revealed by Fig. 8, LB-BSP is the best one among all the schemes, its superiority increasing with the level of heterogeneity. More specifically, in each case, LB-BSP requires the same number of updates for convergence as BSP, and

Instance Type	CPU, Mem (core, GiB)	Num
m4.2xlarge	(8, 32)	17
c5.2xlarge	(8, 16)	10
r4.2xlarge	(8, 61)	2
m4.4xlarge	(16, 64)	2
m4.xlarge	(4, 16)	1

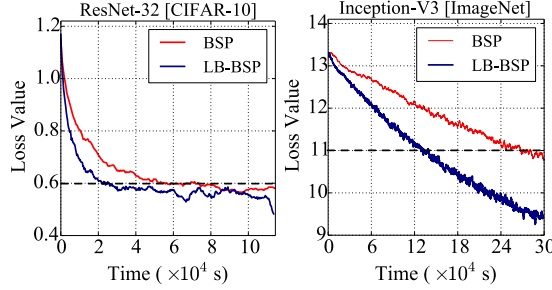


Table 2: Cluster-B composition. **Figure 10: For both models in Cluster-B, convergence speed under LB-BSP is $> 2\times$ of that under BSP.**

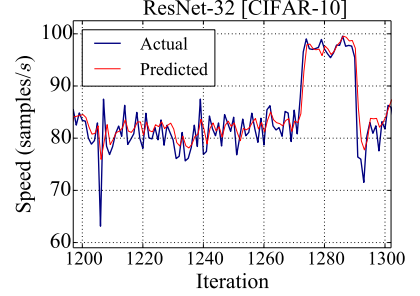


Figure 11: NARX Prediction results on an m4.2xlarge instance in Cluster-B.

meanwhile shares similar average iteration time with ASP (gap $< 5\%$). This indicates that LB-BSP possesses *best statistical efficiency* and *near-optimal hardware efficiency*. From Fig. 8c, at Hetero-L3, LB-BSP outperforms the other schemes by more than 30%.

Meanwhile, we notice that SSP and BSP have similar performance. This is because the stragglers are non-transient under our settings in Cluster-A. As elaborated in §2.2, the staleness threshold under SSP would be easily reached, making fast workers wait for the slowest one almost after each iteration. Furthermore, based on the experiment results of BSP and SSP, we can easily justify that the performance of LB-BSP is better than that of DynSSP. As demonstrated both *theoretically* and *experimentally* in the DynSSP work [44], the statistical performance of DynSSP is *bounded* by BSP, and meanwhile it inherits exactly the *same* hardware efficiency from SSP. In contrast, experiment results confirm that LB-BSP has the *same* statistical efficiency with BSP and *better* hardware efficiency than SSP, so the convergence time under LB-BSP is definitely shorter than that under DynSSP.

ImageNet Results. For ImageNet dataset, we focus on the comparison between LB-BSP and its direct competitor BSP, and run the Inception-V3 model for 3000 iterations under both schemes. After 3000 iterations, we find the loss value are reduced by 15% in both cases, which also confirms that LB-BSP and BSP share the same statistical efficiency.

Regarding the hardware efficiency, the relationship between BSP and LB-BSP, as shown in Fig. 9a, is similar with that of CIFAR-10: the higher the heterogeneity level, the larger the performance improvement from LB-BSP. Particularly, we have measured the average percentage of iteration time that is spent by workers on end-of-iteration waiting. Such percentage represents the portion of computing resources that are wasted, which is what we try to minimize under LB-BSP. As revealed in Fig. 9b, resource wastage under BSP increases saliently with the heterogeneity level, but under LB-BSP it’s quite low ($< 5\%$) in each case.

5.3 Exp. in Emulated Production Cluster

Cluster Setup. To further verify the effectiveness of LB-BSP in production environments, we resort to Cluster-B—an emulated production cluster that is carefully designed based on the released Google traces [57]. Those traces disclosed the machine configurations (CPU/Memory) of a reported Google cluster (in *normalized* form), together with the activities of all the involved jobs/tasks during a selected month—including their resource consumptions and start/end times. When creating Cluster-B, we *scale down* the totally 12,583 machines of that Google cluster to 32 Amazon EC2 instances, with the former’s *hardware heterogeneity proportionally* preserved—by accordingly selecting the EC2 instance types and the instance quantity of each type. Table 2 shows the instance composition of Cluster-B, which actually serves as the *most general* case where each worker machine for the training process is randomly selected from that reported Google cluster.

Meanwhile, we have also emulated the *resource dynamicity* of that Google cluster. For each instance in Cluster-B, we randomly map it to one machine in the Google cluster; during the training process, in that instance we launch a set of faked tasks that share exactly the same start/end times and resource (CPU/memory) consumptions with those submitted to the mapped Google machine.

General performance of LB-BSP. By building up Cluster-B, we are actually emulating the scenarios where a shared-cluster operator utilizes the left-over resources for training DL models in the background. In Cluster-B we respectively train the ResNet-32 and Inception-V3 model for a fixed amount of time. Fig. 10 shows their convergence curves, which are smoothed with a window size of 30 iterations. We find that, given the particular convergence criterion on loss value (0.6 for ResNet-32 and 11.0 for Inception-V3), the convergence speed under LB-BSP is more than $2\times$ of that under BSP for both models. Such a huge improvement suggests it be *highly beneficial* to load-balance DL workloads with LB-BSP in *shared production* clusters.

Method	Configuration	RMSE	Normalized per-update Time
Memoryless	-	11.85	0.584
EMA	$\alpha=0.2$	7.85	0.489
ARIMA	$(p,d,q)=(2,2,1)$	9.67	0.523
SimpleRNN	look-back=2	8.34	0.491
LSTM	look-back=2	9.19	0.515
NARX	look-back=2	4.78	0.423

Table 3: RMSE and normalized per-update time when applying different prediction approaches in LB-BSP.

5.4 Deep Dive into NARX Performance

Accurate sample processing speed prediction is crucial for the performance of LB-BSP. As elaborated in Sec. 3.2.1, we have resorted to the NARX model for speed prediction. Then, how on earth does the NARX approach perform? We answer that by diving deep into the speed prediction results in the above experiments conducted in Cluster-B.

Visual analysis. To get a *visual* understanding of NARX prediction performance, we randomly select a period (iteration 1200~1300) from the ResNet-32 training process on one m4.2xlarge instance of Cluster-B; the *actual* and *predicted* sample processing speeds are presented in Fig. 11. From it we observe that the benefit of NARX is twofold. On the one hand, NARX is robust to *transient* perturbations: when there are “spikes” (like the sharp wave around iteration 1206) in the actual speed curve, the predicted curve fluctuates much less. This is because NARX predicts also with the worker’s available memory and CPU amounts, which are relatively stable during those “spikes”. On the other hand, when the actual speed increases not for randomness but for *non-transient deterministic* factors like increased CPU/memory resources (e.g., around iteration 1270), the predicted speed can *promptly* catch up with the actual speed.

Comparison with other approaches. We further compare NARX with other approaches we surveyed in §3.2.1, as listed in Table. 3. Here the *memoryless* method means to simply take last iteration’s sample processing speed as the predicted one. Regarding the EMA approach, the smoothing factor α (weight of the latest observation) is set to be 0.2. As for the statistical prediction approach—ARIMA, its *order of the autoregressive model* (p), *degree of differencing* (d), and *order of the moving average* (q) are respectively set to 2, 2 and 1, based on its model selection techniques [54]. Finally, for SimpleRNN (plain RNN) and LSTM, their *look-back* window size is set to 2, the same as in NARX.

Then, we replace the NARX approach respectively with each of those prediction approaches when training ResNet-32 model under LB-BSP in Cluster-B. For each approach, we record the average *root-mean-square error* (RMSE) of the prediction results, as well as the corresponded per-update time (*normalized* by the per-update time under BSP). From

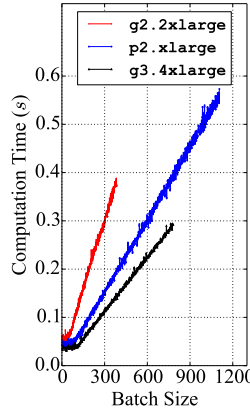


Figure 12: $\Gamma(\cdot)$ (§3.1) for GPU-instances in Cluster-C.

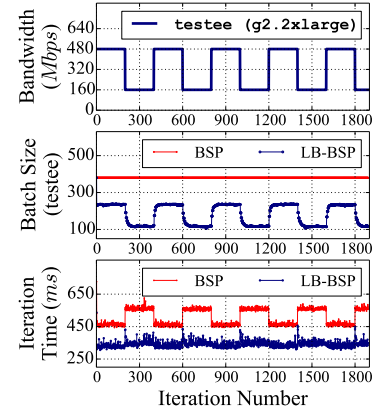


Figure 13: Performance of BSP/LB-BSP facing network variations in Cluster-C.

the results in Table. 3, the NARX approach, due to its ability to perceive CPU/memory resource variations, can do the best among all those candidates—it surpasses the second best by around 40% in RMSE and 15% in per-update time.

5.5 Micro-benchmarks in GPU Cluster

Cluster Setup. We resort to **Cluster-C** to verify the effectiveness of LB-BSP in GPU-clusters. Cluster-C contains 8 single-GPU workers: *four* g2.2xlarge instances (with a NVIDIA GRID K520 GPU), *two* p2.xlarge instances (with a NVIDIA Tesla K-80 GPU), and *two* g3.4xlarge instances (with a NVIDIA Tesla M60 GPU). Each worker is installed with CUDA-8.0 and cuDNN-5. Meanwhile, the DL model trained is ResNet-32 (on CIFAR-10 dataset), and the initial batch size is 380. For generality, in Cluster-C the deployed DL framework is switched to MXNet.

Fig. 12 shows the profiled relationships between computation time and batch size, i.e., $\Gamma(\cdot)$, for the three GPU instance types in Cluster-C, which are consistent with our observations in Fig. 6 (§3.3). In particular, the $[x^s, x^o]$ pairs of g2.2x, p2.x and g3.4x instances are [58, 384], [92, 1184] and [103, 788], respectively.

Recall that LB-BSP in GPU-clusters can react to hardware heterogeneity and network variations. To verify that, we select one g2.2x worker as the testee, and periodically rotate its link bandwidth (with Wonder Shaper [12]) between an *abundant* state (480Mbps) and a *deficient* state (160Mbps). For performance comparison between LB-BSP and BSP, we record the testee’s temporal batch size and the corresponded iteration time, as shown in Fig. 13.

LB-BSP outperforms BSP in two aspects. First, in face of the hardware (GPU) heterogeneity, LB-BSP sets each worker’s batch size based on their computing capabilities: the batch size of the g2.2xlarge instances is adjusted from 380 to 235

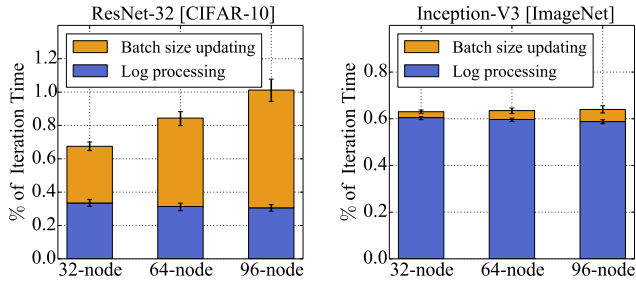


Figure 14: LB-BSP Overhead breakdown.

to compensate for their relatively low speeds. This brings a performance improvement of around 27%. Second, when the testee’s bandwidth drops, its prolonged communication time would be perceived under LB-BSP (with EMA), which further reduces its batch size as a remediation. This limits the negative influence of bandwidth drop to less than 3%. As a result, compared with BSP, LB-BSP improves the hardware efficiency by totally more than 41%.

5.6 System Overhead and Scalability

In TensorFlow, the worker overheads brought by LB-BSP come from two perspectives. First, to get the sample processing speed in an iteration, we need to process the worker execution logs (Timeline object). Besides, each worker shall communicate with the BatchSizeManager to get the updated batch size. For CPU-clusters, both processes are *blocking* (§4) and would take extra time in each iteration. Next, we measure those overheads at different cluster scales.

We respectively train ResNet-32 and Inception-V3 model for 1000 iterations in three clusters—first Cluster-A, then its *enlarged* versions with *doubled/tripled* size. Fig. 14 shows the average time respectively spent on log processing and batch size updating, *normalized* by the iteration time. Here the error bars show the 5th/95th percentile. Even in the largest cluster with 96 workers, the total overheads are less than 1.1% of the iteration time for both models—such a cost (*slowdown*) is much less compared with the benefit (*speedup*) from LB-BSP.

Besides, we also confirm that performance of the PS is almost not affected by the co-located BatchSizeManager: we migrate the BatchSizeManager to a dedicated machine, and again train ResNet-32 in the 96-worker cluster. Our measurements show that, without BatchSizeManager, the *push/pull* interactions between the PS and workers are sped up merely by 1.3% on average. So there is no need to provision extra machine for BatchSizeManager.

6 RELATED WORK

Straggler Treatment. Stragglers have long been an annoying problem for parallel computing; basically the cures are of two kinds: *load balancing* and *redundant execution*.

Load balancing is the most *fundamental* methodology to solve the straggler problem. In traditional multi-core systems [14, 17, 33], *work stealing* has been exploited to balance the loads among different computing cores: once a core becomes idle, it will steal work from other busy ones. Recently, FlexRR [38] was proposed for load balancing in data-parallel iterative Machine Learning frameworks; it combines SSP with an intra-iteration work reassignment mechanism. As justified in §2.3, such fine-grained techniques do not fit DL workloads.

Redundant execution [15, 66] is typically adopted to mitigate stragglers in data analytics frameworks like MapReduce and Spark, and it works by *speculatively* launching multiple copies of the straggling tasks and picking up only the one finishing earliest. Recently, it has been also applied in distributed learning systems: Chen *et al.* [20] have proposed to train DL models with *backup workers* and use gradients from those finishing earlier. However, all those approaches are *suboptimal*: they merely *mitigate* the worst stragglers instead of *fundamentally eliminating* all the progress inconsistency; worse, they waste extra computing resources.

Batching Manipulation. Batching is necessary when the input is a long-lasting stream or too large to be processed all at once. In real-time streaming systems [61, 65], improper batching interval (*size* or *time*) would cause either *low throughput* or *long end-to-end latency*. Thus, some works [27, 68] have explored how to adaptively adjust the batching interval when faced with dynamic data rates or operating conditions. Yet, such adjustments focus only at the *front-end* batching interface, without involving the *back-end* parallel workers. Meanwhile, from an algorithmic perspective of DL, some [28, 31] have proposed to adaptively increase the batch size during the training process to yield faster convergence; those works are orthogonal to ours. To the best of our knowledge, we are the first that has identified the superiority of and then leveraged *coordinated batch size tuning* to load-balance different workers in the distributed DL training process.

7 CONCLUSION

In this work, we presented LB-BSP, an adaptive mechanism that improves the performance of distributed deep learning training by apportioning the workload to each worker according to its processing capability. Called worker-adaptive batch sizing, we mathematically formulate the problem as an optimization problem, and solve it for CPU-clusters and GPU-clusters, respectively. In particular, we employ a NARX model to predict the processing speed of workers in CPU-clusters. We have implemented LB-BSP as a Python library and integrated it into both TensorFlow and MXNet, two of the modern and most popular deep learning frameworks. Our extensive experiments have shown that it is able to outperform BSP by 2×.

REFERENCES

- [1] Apache Thrift. <https://thrift.apache.org/>.
- [2] EC2 Spot Instances. <https://aws.amazon.com/ec2/spot/>.
- [3] GPU sharing is not supported in TensorFlow. <https://github.com/tensorflow/tensorflow/issues/2210>.
- [4] GPU sharing is rare in practice. <https://www.quora.com/Can-I-run-multiple-deep-learning-models-on-the-same-GPU/>.
- [5] Keras. <https://keras.io/>.
- [6] Python Psutil. <https://psutil.readthedocs.io/en/latest/>.
- [7] Python Threading2. <https://pypi.python.org/pypi/threading2>.
- [8] Stress-ng: a tool to load and stress a computer system. <http://manpages.ubuntu.com/manpages/artful/man1/stress-ng.1.html>.
- [9] TensorFlow Inception-V3. <https://github.com/tensorflow/models/tree/master/research/inception>.
- [10] TensorFlow Models in Official Github Repository. <https://github.com/tensorflow/models>.
- [11] TensorFlow Timeline. <https://github.com/tensorflow/tensorflow/blob/master/tensorflow/python/client/timeline.py>.
- [12] Wonder Shaper. <https://github.com/chenc10/wondershaper>.
- [13] Martín Abadi et al. 2016. TensorFlow: A System for Large-Scale Machine Learning. In *USENIX OSDI*.
- [14] Umut A Acar, Arthur Charguéraud, and Mike Rainey. 2013. Scheduling parallel programs by work stealing with private dequeues. In *ACM SIGPLAN Notices*.
- [15] Ganesh Ananthanarayanan, Ali Ghodsi, Scott Shenker, and Ion Stoica. 2013. Effective Straggler Mitigation: Attack of the Clones.. In *USENIX NSDI*.
- [16] Dimitrios Argyropoulos, Dimitris S Paraforos, Rainer Alex, Hans W Griepentrog, and Joachim Müller. 2016. NARX neural network modelling of mushroom dynamic vapour sorption kinetics. *IFAC-PapersOnLine* 49, 16 (2016), 305–310.
- [17] Robert D Blumofe and Charles E Leiserson. 1999. Scheduling multi-threaded computations by work stealing. *JACM* 46, 5 (1999), 720–748.
- [18] Richard H Byrd, Gillian M Chin, Jorge Nocedal, and Yuchen Wu. 2012. Sample size selection in optimization methods for machine learning. *Mathematical programming* 134, 1 (2012), 127–155.
- [19] Erasmo Cadenas, Wilfrido Rivera, Rafael Campos-Amezcuca, and Roberto Cadenas. 2016. Wind speed forecasting using the NARX model, case: La Mata, Oaxaca, México. *Neural Computing and Applications* 27, 8 (2016), 2417–2428.
- [20] Jianmin Chen, Rajat Monga, Samy Bengio, and Rafal Jozefowicz. 2016. Revisiting distributed synchronous SGD. *arXiv preprint arXiv:1604.00981* (2016).
- [21] Tianqi Chen, Mu Li, Yutian Li, Min Lin, Naiyan Wang, Minjie Wang, Tianjun Xiao, Bing Xu, Chiyuan Zhang, and Zheng Zhang. 2015. Mxnet: A flexible and efficient machine learning library for heterogeneous distributed systems. *arXiv preprint arXiv:1512.01274* (2015).
- [22] Trishul Chilimbi, Yutaka Suzue, Johnson Apacible, and Karthik Kalyanaraman. 2014. Project adam: Building an efficient and scalable deep learning training system. In *USENIX OSDI*.
- [23] Ronan Collobert, Jason Weston, Léon Bottou, Michael Karlen, Koray Kavukcuoglu, and Pavel Kuksa. 2011. Natural language processing (almost) from scratch. *J. Mach. Learn. Res.* 12, Aug (2011), 2493–2537.
- [24] Jerome T Connor, R Douglas Martin, and Les E Atlas. 1994. Recurrent neural networks and robust time series prediction. *IEEE Trans. on Neural Networks* 5, 2 (1994), 240–254.
- [25] Eli Cortez, Anand Bonde, Alexandre Muzio, Mark Russinovich, Marcus Fontoura, and Ricardo Bianchini. 2017. Resource Central: Understanding and Predicting Workloads for Improved Resource Management in Large Cloud Platforms.
- [26] Henggang Cui, James Cipar, Qirong Ho, Jin Kyu Kim, Seunghak Lee, Abhimanu Kumar, Jinliang Wei, Wei Dai, Gregory R Ganger, Phillip B Gibbons, et al. 2014. Exploiting Bounded Staleness to Speed Up Big Data Analytics. In *USENIX ATC*.
- [27] Tathagata Das, Yuan Zhong, Ion Stoica, and Scott Shenker. 2014. Adaptive stream processing using dynamic batch sizing. In *ACM SoCC*.
- [28] Soham De, Abhay Yadav, David Jacobs, and Tom Goldstein. 2017. Automated inference with adaptive batches. In *Artificial Intelligence and Statistics*. 1504–1513.
- [29] Jeffrey Dean, Greg Corrado, Rajat Monga, Kai Chen, Matthieu Devin, Mark Mao, Andrew Senior, Paul Tucker, Ke Yang, Quoc V Le, and Andrew Ng. 2012. Large scale distributed deep networks. In *NIPS*.
- [30] Jeffrey Dean and Sanjay Ghemawat. 2010. MapReduce: a flexible data processing tool. *Commun. ACM* 53, 1 (2010), 72–77.
- [31] Aditya Devarakonda, Maxim Naumov, and Michael Garland. 2017. AdaBatch: Adaptive Batch Sizes for Training Deep Neural Networks. *arXiv preprint arXiv:1712.02029* (2017).
- [32] Eugen Diaconescu. 2008. The use of NARX neural networks to predict chaotic time series. *Wseas Transactions on computer research* 3, 3 (2008), 182–191.
- [33] James Dinan, D Brian Larkins, Ponnuswamy Sadayappan, Sriram Krishnamoorthy, and Jarek Nieplocha. 2009. Scalable work stealing. In *IEEE/ACM SC*.
- [34] Volkan Ş Ediger and Sertac Akar. 2007. ARIMA forecasting of primary energy demand by fuel in Turkey. *Energy Policy* 35, 3 (2007), 1701–1708.
- [35] Clement Farabet, Camille Couprie, Laurent Najman, and Yann LeCun. 2013. Learning hierarchical features for scene labeling. *IEEE Trans. Pattern Anal. Mach. Intell.* 35, 8 (2013), 1915–1929.
- [36] Yang Gao and Meng Joo Er. 2003. NARMAX-model-based time series modeling and prediction: feedforward and recurrent fuzzy neural network approaches. In *WSEAS CSECS*.
- [37] Priya Goyal, Piotr Dollár, Ross Girshick, Pieter Noordhuis, Lukasz Wesolowski, Aapo Kyrola, Andrew Tulloch, Yangqing Jia, and Kaiming He. 2017. Accurate, Large Minibatch SGD: Training ImageNet in 1 Hour. *arXiv preprint arXiv:1706.02677* (2017).
- [38] Aaron Harlap, Henggang Cui, Wei Dai, Jinliang Wei, Gregory R Ganger, Phillip B Gibbons, Garth A Gibson, and Eric P Xing. 2016. Addressing the straggler problem for iterative convergent parallel ML. In *ACM SoCC*.
- [39] Kaiming He, Xiangyu Zhang, Shaoqing Ren, and Jian Sun. 2016. Deep residual learning for image recognition. In *IEEE CVPR*.
- [40] Vishakh Hegde and Sheema Usmani. 2016. *Parallel and Distributed Deep Learning*. Technical Report. Tech. report, Stanford University, June 2016. https://stanford.edu/~rezab/dao/projects_reports/hedge_usmani.pdf.
- [41] Qirong Ho, James Cipar, Henggang Cui, Seunghak Lee, Jin Kyu Kim, Phillip B Gibbons, Garth A Gibson, Greg Ganger, and Eric P Xing. 2013. More effective distributed ml via a stale synchronous parallel parameter server. In *NIPS*.
- [42] Sepp Hochreiter and Jürgen Schmidhuber. 1997. Long short-term memory. *Neural computation* 9, 8 (1997), 1735–1780.
- [43] Yangqing Jia, Evan Shelhamer, Jeff Donahue, Sergey Karayev, Jonathan Long, Ross Girshick, Sergio Guadarrama, and Trevor Darrell. 2014. Caffe: Convolutional architecture for fast feature embedding. In *ACM Multimedia*.
- [44] Jiawei Jiang, Bin Cui, Ce Zhang, and Lele Yu. 2017. Heterogeneity-aware distributed parameter servers. In *ACM SIGMOD*.
- [45] Alex Krizhevsky and Geoffrey Hinton. 2009. Learning multiple layers of features from tiny images. (2009).
- [46] Alex Krizhevsky, Ilya Sutskever, and Geoffrey E Hinton. 2012. ImageNet classification with deep convolutional neural networks. In

- NIPS*.
- [47] John Langford, Alexander J Smola, and Martin Zinkevich. 2009. Slow learners are fast. In *NIPS*.
 - [48] Yann LeCun, Yoshua Bengio, and Geoffrey Hinton. 2015. Deep learning. *Nature* 521, 7553 (2015), 436–444.
 - [49] Ang Li. 2016. *GPU performance modeling and optimization*. Ph.D. Dissertation. Technische Universiteit Eindhoven.
 - [50] Mu Li, David G Andersen, Jun Woo Park, Alexander J Smola, Amr Ahmed, Vanja Josifovski, James Long, Eugene J Shekita, and Bor-Yiing Su. 2014. Scaling Distributed Machine Learning with the Parameter Server. In *USENIX OSDI*.
 - [51] Mu Li, Tong Zhang, Yuqiang Chen, and Alexander J Smola. 2014. Efficient mini-batch training for stochastic optimization. In *ACM KDD*.
 - [52] Alberto Magni, Christophe Dubach, and Michael O’Boyle. 2014. Exploiting GPU hardware saturation for fast compiler optimization. In *ACM GPGPU*.
 - [53] Chen Meng, Minmin Sun, Jun Yang, Minghui Qiu, and Yang Gu. 2017. Training Deeper Models by GPU Memory Optimization on TensorFlow. In *ML Systems Workshop in NIPS*.
 - [54] T Ozaki. 1977. On the order determination of ARIMA models. *Applied Statistics* (1977), 290–301.
 - [55] Nicholas G Polson and Vadim O Sokolov. 2017. Deep learning for short-term traffic flow prediction. *Transportation Research Part C: Emerging Technologies* 79 (2017), 1–17.
 - [56] Akhter Mohiuddin Rather, Arun Agarwal, and VN Sastry. 2015. Recurrent neural network and a hybrid model for prediction of stock returns. *Expert Systems with Applications* 42, 6 (2015), 3234–3241.
 - [57] Charles Reiss, Alexey Tumanov, Gregory R Ganger, Randy H Katz, and Michael A Kozuch. 2012. Heterogeneity and dynamicity of clouds at scale: Google trace analysis. In *ACM SoCC*.
 - [58] Olga Russakovsky, Jia Deng, Hao Su, Jonathan Krause, Sanjeev Satheesh, Sean Ma, Zhiheng Huang, Andrej Karpathy, Aditya Khosla, Michael Bernstein, Alexander C. Berg, and Li Fei-Fei. 2015. ImageNet Large Scale Visual Recognition Challenge. *International Journal of Computer Vision (IJCV)* 115, 3 (2015), 211–252. <https://doi.org/10.1007/s11263-015-0816-y>.
 - [59] Ilya Sutskever, Oriol Vinyals, and Quoc V Le. 2014. Sequence to sequence learning with neural networks. In *NIPS*.
 - [60] Christian Szegedy, Wei Liu, Yangqing Jia, Pierre Sermanet, Scott Reed, Dragomir Anguelov, Dumitru Erhan, Vincent Vanhoucke, Andrew Rabinovich, et al. 2015. Going deeper with convolutions. In *IEEE CVPR*.
 - [61] Ankit Toshniwal, Siddarth Taneja, Amit Shukla, Karthik Ramasamy, Jignesh M Patel, Sanjeev Kulkarni, Jason Jackson, Krishna Gade, Maosong Fu, Jake Donham, et al. 2014. Storm@ twitter. In *ACM SIGMOD*.
 - [62] Linnan Wang, Jinmian Ye, Yiyang Zhao, Wei Wu, Ang Li, Shuaiwen Leon Song, Zenglin Xu, and Tim Kraska. 2018. SuperNeurons: Dynamic GPU Memory Management for Training Deep Neural Networks. In *ACM PPoPP*.
 - [63] Yang Yang, De-Chuan Zhan, Ying Fan, Yuan Jiang, and Zhi-Hua Zhou. 2017. Deep Learning for Fixed Model Reuse. In *AAAI* 2831–2837.
 - [64] Matei Zaharia, Mosharaf Chowdhury, Tathagata Das, Ankur Dave, Justin Ma, Murphy McCauley, Michael J Franklin, Scott Shenker, and Ion Stoica. 2012. Resilient distributed datasets: A fault-tolerant abstraction for in-memory cluster computing. In *USENIX NSDI*.
 - [65] Matei Zaharia, Tathagata Das, Haoyuan Li, Timothy Hunter, Scott Shenker, and Ion Stoica. 2013. Discretized streams: Fault-tolerant streaming computation at scale. In *ACM SOSP*.
 - [66] Matei Zaharia, Andy Konwinski, Anthony D Joseph, Randy H Katz, and Ion Stoica. 2008. Improving MapReduce performance in heterogeneous environments. In *USENIX OSDI*.
 - [67] Hao Zhang, Zeyu Zheng, Shizhen Xu, Wei Dai, Qirong Ho, Xiaodan Liang, Zhiting Hu, Jinliang Wei, Pengtao Xie, and Eric P Xing. 2017. Poseidon: An Efficient Communication Architecture for Distributed Deep Learning on GPU Clusters. In *USENIX ATC*.
 - [68] Quan Zhang, Yang Song, Ramani R Routray, and Weisong Shi. 2016. Adaptive block and batch sizing for batched stream processing system. In *IEEE ICAC*.